

AD-A276 705



2

OFFICE OF NAVAL RESEARCH

Contract No. N00014-91-J-1409

Technical Report No. 144

Influence of Adsorbed Hydroxyl and Carbon Monoxide  
on Potential-Induced Reconstruction of Au(100)  
as Examined by Scanning Tunneling Microscopy

DTIC  
ELECTE  
MAR 10 1994  
S F D

by

G.J. Edens, X. Gao, and M.J. Weaver

Department of Chemistry, Purdue University  
West Lafayette, Indiana 47907

N.M. Markovic and P.N. Ross

Materials Sciences Division, Lawrence Berkeley Laboratory  
One Cyclotron Road, Berkeley, California 94720

Prepared for Publication

in

Surface Science Letters

94-07839



February 1994

Reproduction in whole, or in part, is permitted for any purpose of the United States Government.

\* This document has been approved for public release and sale; its distribution is unlimited.

94 3 9 094

**Best  
Available  
Copy**

**ABSTRACT**

The potential-dependent hexagonal ("hex") reconstruction of ordered Au(100) in an alkaline electrolyte, 0.1 M KOH, has been examined by means of in-situ scanning tunneling microscopy. In harmony with recent X-ray diffraction results, the hex  $\rightarrow$  (1  $\times$  1) transition occurs at lower potentials, ca 0 V vs SCE, than in weakly adsorbing acidic media such as perchloric acid, consistent with an influence of hydroxide adsorption. The dynamics of the reverse (1  $\times$  1)  $\rightarrow$  hex transition accelerate markedly as the potential is lowered below ca -0.35 V vs SCE. Carbon monoxide adsorption, induced in 0.1 M KOH at negative potentials, facilitates the *formation* of a notably homogeneous hex phase.

Accession For	
NTIS	CRA&I
DTIC	TAB
Unannounced	
Justification	
By	
Distribution/	
Availability Codes	
Dist	Avail and/or Special
A-1	

The last 2-3 years have witnessed substantial advances in our knowledge of metal reconstruction in electrochemical systems, primarily for low-index gold surfaces in aqueous media.<sup>1,2</sup> These ongoing developments have been driven by the concurrent emergence of new in-situ structural probes, most notably scanning tunneling microscopy (STM) and surface X-ray scattering (SXRS). While these new techniques are markedly different in character and exhibit contrasting strengths and weaknesses, both are providing information on atomic structure for metal-solution interfaces which is now on a par with that obtained for surfaces in ultrahigh vacuum (uhv). Of the various surfaces examined by STM and SXRS so far, Au(100) is of particular interest.<sup>3-7</sup> As for other low-index gold surfaces, reconstruction can be formed or removed by applying electrode potentials corresponding to negative or positive electronic charge densities, respectively. For Au(100), the transition between the hexagonal reconstructed ("hex") and (1 × 1) phases observed under these conditions involves a substantial (ca 24%) change in surface metal atomic density. The potential-dependent dynamics of this hex ↔ (1 × 1) conversion, and the attendant surface mass transfer, constitute questions of broadbased fundamental significance.

These issues are enriched by the observed sensitivity of both the electrochemical thermodynamics and dynamics of the hex ↔ (1 × 1) conversion to the nature of the electrolyte anion.<sup>3,4,6,8</sup> Specific anion adsorption both shifts the "equilibrium potential" of the hex ↔ (1 × 1) transition to lower (i.e. less positive) values, and can enhance considerably the conversion dynamics. Detailed information on the latter issue can be revealed by STM, especially image sequences obtained under potentiodynamic conditions.<sup>6</sup>

Of interest in this regard is the behavior of Au(100) in alkaline as well as acidic electrolytes. Hydroxide ions commonly yield dramatic changes in metal surface oxidation and also electrocatalytic properties. Two of us recently

reported a detailed SXRS study of Au(100) reconstruction in alkaline (0.1 M KOH) in comparison with perchloric acid electrolytes.<sup>4</sup> Substantial differences were observed in both the potential-dependent structures and dynamics which can be attributed to the influence of OH<sup>-</sup> adsorption.

We report here an examination by in-situ STM of Au(100) reconstruction in 0.1 M KOH, employing similar tactics to a recent detailed study undertaken in acidic electrolytes.<sup>6a</sup> Besides enabling a comparison to be made between parallel STM and SXRS results in alkaline versus acidic media, the findings shed some light on the role of adsorbed OH<sup>-</sup>. We also report a notable influence of adsorbed carbon monoxide on facilitating the formation of the hex reconstruction.

The experimental STM procedures were largely as described elsewhere.<sup>5,6</sup> The microscope is a Nanoscope II (Digital Instruments) with a bipotentiostat for in-situ electrochemical STM. The STM tips were Ir wires, sharpened by mechanical polishing and insulated by means of a thermosetting plastic as dispensed by a commercial (Sears) "glue gun."<sup>6a</sup> This strategy largely avoided surface contamination by the tip insulating material even in the present alkaline electrolyte, as evidenced from cyclic voltammetry (vide infra). The tip potential was typically held around 0 V vs SCE, with the tunneling currents in the range 5-10 nA. The Au(100) crystal pretreatment employed here involved flame annealing followed by cooling in a flowing hydrogen stream (as in ref. 4), and transferring to the STM cell protected by a drop of water. The reference electrode in the STM cell was a H<sub>2</sub>-charged Pd wire;<sup>4</sup> the potentials quoted here (reliable to  $\pm 50$  mV), however, are versus the saturated calomel electrode (SCE).

The upper part of Fig. 1 contains a representative cyclic voltammogram at 50 mV s<sup>-1</sup>, encompassing the negative potential and gold oxidation regions, for Au(100) in 0.1 M KOH, obtained in a conventional electrochemical cell (solid trace). The voltammetric features, consistent with earlier reports,<sup>4,9</sup> include

the usual hysteretic peaks associated with oxide formation and reduction at positive potentials. The lower part of Fig. 1 shows a cyclic voltammogram obtained under similar conditions, but in the STM cell. The close similarity in these voltammograms attests to the surface cleanliness achieved under working STM conditions, even though an additional cathodic peak is evident in the lower trace, due to reduction of dissolved oxygen.

A significant feature on both voltammograms is the peak labelled  $C_p$ , appearing at about 0 V vs SCE during the positive-going sweep. This component, which is enlarged progressively by holding the potential at more negative values for several minutes, was suggested to be due to potential-induced lifting of reconstruction<sup>9</sup> by analogy with related peaks observed for Au(100) in acidic media.<sup>8</sup> Potentiodynamic STM data, i.e. images acquired during suitable voltammetric potential excursions, have confirmed that  $C_p$  arises from a sharp hex  $\rightarrow$  (1  $\times$  1) phase transition.<sup>6</sup> Evidence pointing to the same conclusion in the present alkaline medium has been obtained by X-ray reflectivity measurements.<sup>4</sup>

Following the annealing pretreatment, STM images obtained for Au(100) in air showed the presence of large (ca 50 nm) ordered (1  $\times$  1) as well as hex domains. (In this regard, then, the present flame annealing-hydrogen cooling procedure yields surfaces that are apparently intermediate in character between those formed by cooling in water and in air,<sup>6a</sup> although typically providing larger ordered domains.) The (1  $\times$  1) surface regions are characterized by a square-planar array of gold atoms, spaced 2.9 Å apart.<sup>5</sup> The hex reconstruction can readily be detected by STM, even for large surface regions without true atomic resolution, from the characteristic corrugated strings, spaced 14.5 Å apart, that arise from the periodic undulations in binding site between the hexagonal top layer and underlying square-planar substrate across the short dimension of the ("5  $\times$  20") [more precisely<sup>5b</sup> (5  $\times$  27)] unit cell. Figures 2A

and B show typical examples of these  $(1 \times 1)$  and hex structural features, respectively, as characterized by in-situ STM in the present 0.1 M KOH environment. The former atomic-resolution image was acquired at 0.2 V vs SCE after sweeping the potential from negative values, whereas the latter image was obtained at -0.6 V after holding the potential for several minutes. The presence of corrugated strands running roughly parallel to both  $(110)$  substrate directions is evident, as is the variability of the precise row alignment by at least  $10^\circ$  or so. This "flexibility" of the hex structural orientation with respect to the substrate is a hallmark of electrochemically induced reconstruction on Au(100) in several electrolytes, especially for small terraces and/or in the vicinity of surface defects.<sup>5b,6</sup>

Of concern here are the dynamics of propagating the potential-induced reconstruction in the present alkaline medium with respect to other, especially acidic, electrolytes. Selected members of a sequence of STM images showing sequential potential-induced forming and removing the Au(100) hex reconstruction in 0.1 M KOH are shown in Figs. 3A-D. Image A was recorded at -0.35 V following a cyclic voltammogram to 0.8 V and back to 0 V, then a slow ( $5 \text{ mV s}^{-1}$ ) sweep to -0.35 V. The large single-atom deep pits on the  $(1 \times 1)$  terrace that encompass most of the imaged area were formed during the preceding surface oxidation/reduction process.<sup>10</sup> A few narrow "strings" are also evident in A, running parallel to both  $(110)$  substrate directions ( $90^\circ$  to each other). As detailed in earlier reports,<sup>5b,6a</sup> these strings consist of at least one additional gold atomic row embedded in the otherwise  $(1 \times 1)$  terrace and packing hexagonally with the adjacent substrate atoms. These long hex "microdomains" appear to propagate from terrace edge sites, which may act as nucleation centers and/or sources of the extra gold atoms required. Also discernable in Fig. 3A, however, are a number of "micropits" formed alongside some of the strings,

betraying an additional source of these atoms.

Figure 3B, which was recorded at  $-0.35$  V about 1 min after A, shows a substantial development of the hex microdomains, increasing both in breadth and density. The rate of initial string growth as seen in these and other images in  $0.1$  M KOH at ca  $-0.3$  to  $-0.4$  V is similar to that observed in  $0.1$  M HClO<sub>4</sub> at these potentials,<sup>6a</sup> suggesting that any residual OH<sup>-</sup> adsorption is not playing a major role in the reconstruction dynamics. A subtle yet significant difference between the STM data in the alkaline and acidic media, however, is that the strings tend to be initially broader for the former electrolyte, typically 6-18 versus 3-6 atoms across, respectively. This difference may reflect a larger local availability of the gold adatoms required for reconstruction in  $0.1$  M KOH.

An interesting aspect of the Au(100)-alkaline system is that substantially more negative potentials can be accessed prior to hydrogen evolution than in acidic media, enabling the influence of increasing the electrochemical driving force on the reconstruction dynamics to be explored to a greater extent. Figure 3C shows the same imaged area as in A and B, but about 1 min after altering the potential to  $-0.7$  V. (More negative potentials yielded less stable images, probably due to undesirable tip electrochemistry.) The surface is now seen to be extensively reconstructed, with a dense "criss-cross" pattern of hexagonal strings, that eventually coalesce into uniform hex domains. The hex formation rate at  $-0.7$  V is clearly markedly faster than at  $-0.35$  V. Intercomparison of Figs. 3A-C sheds some light on the real-space reconstruction dynamics. A notable feature is the increasing size and altered shape of the pits with hex phase development. The driving force is presumably the markedly increased coordination number as the atoms move from terrace edge to hex terrace sites. The long terrace edge running diagonally towards the upper right-hand side of the imaged area becomes more "jagged" following reconstruction, indicating selective loss

of atoms at such step sites. Interestingly, the narrow lower terrace running just below this long terrace edge exhibits hex strings running largely *parallel* to the monoatomic step. This can be anticipated from the ease of fueling the growth of such strings from atoms breaking away from the nearby upper terrace edge (cf ref. 5b).

The relatively slow kinetics of hex phase growth as discerned by STM is consistent with SXRS data obtained under similar conditions,<sup>4</sup> although the former affords more direct real-space detail. This observation also has implications for the electroreduction of  $O_2$  on Au(100) in 0.1 M KOH. This reaction is seen to proceed via a predominantly four-electron pathway in the potential region, positive of ca -0.2 V, where the  $(1 \times 1)$  phase is stable, yet follows a two-electron pathway (yielding peroxide) at more negative potentials.<sup>4b,11</sup> Significantly, the potential-induced alteration between the four- and two-electron pathways can be made to occur substantially more rapidly than the time required for the  $(1 \times 1) \rightarrow$  hex conversion.<sup>4b</sup> This observation implies that the  $(1 \times 1) \rightarrow$  hex phase transition is *not* responsible (at least not alone) for the change in the  $O_2$  reduction mechanism. Rather, the occurrence of the four-electron pathway is likely to be triggered by the presence of adsorbed hydroxyl, as suggested earlier;<sup>11</sup> this species will be rapidly desorbed at more negative potentials, initiating the *slower*  $(1 \times 1) \rightarrow$  hex phase transition.

As anticipated above, potentiodynamic STM measurements recorded subsequently on Au(100) in 0.1 M KOH during positive-going sweeps at  $10 \text{ mV s}^{-1}$  sweeps showed essentially complete removal of the hex domains within the narrow (ca 50–70 mV) potential range encompassing  $C_p$  (Fig. 1). Figure 3D shows an image obtained following Figs. 3A–C, by sweeping the potential positive to a point just beyond  $C_p$ . The ca 24% excess atoms released by lifting the hex reconstruction are seen to collect into arrays of  $(1 \times 1)$  clusters. The initial average sizes

of the clusters, 5–10 nm, are comparable to those obtained in 0.1 M  $\text{H}_2\text{SO}_4$ , but larger than in 0.1 M  $\text{HClO}_4$ .<sup>6a,b</sup> As in these acidic media, the cluster islands formed in 0.1 M  $\text{KOH}$  tend to aggregate with time, the average size being 10–15 nm after 5 min. Reforming the hex reconstruction by subsequent negative potential excursions to  $-0.2$  V or beyond resulted in virtually complete removal of the clusters, these features thereby acting as a major source of the additional atoms required for the next  $(1 \times 1) \rightarrow \text{hex}$  transition.

An interesting and somewhat surprising feature of gold in aqueous, especially alkaline, electrolytes is the formation of moderate or even high coverages of irreversibly adsorbed carbon monoxide by solution CO dosing.<sup>12,13</sup> The adsorbed CO, which is most prevalent on Au(210) and other high-index surfaces, yields an infrared spectral fingerprint (C–O stretch at  $1900\text{--}2000\text{ cm}^{-1}$ ) consistent with bridge bonding. This adsorbed CO is quite distinct from the atop coordinated form (C–O stretch at  $2100\text{--}2130\text{ cm}^{-1}$ ) which acts as the intermediate for solution CO electrooxidation on gold; indeed the former adsorbate is instead an *inhibitor* for this reaction.<sup>13,14</sup> Although this bridge-bonded CO is produced to a smaller extent on Au(100) than on (210), and extensively only at negative potentials (below ca 0 V vs SCE), its presence nevertheless exerts a surprising influence on the potential-dependent Au(100) reconstruction.

As an example, holding the potential at  $-0.1$  V (i.e. at or close to  $C_p$ ) in 0.1 M  $\text{KOH}$  yields essentially a stable  $(1 \times 1)$  surface. Dosing CO into the STM cell, undertaken most conveniently by flushing CO gas into the surrounding chamber at about  $-0.1$  V or more negative potentials, however, yielded some *reformation* of the hex construction within 10 mins or so. While extensive reconstruction can be induced at potentials negative of  $-0.35$  V in 0.1 M  $\text{KOH}$  (vide supra), the addition of CO yields the facile production of uniform hex domains as discerned by STM. Figures 4A and B show illustrative STM images of

such regions. The former (A) shows upper and lower terraces, both with hex domains running in only one direction; the upper hex terraces are seen to be formed by gold atom transfer from the lower terrace. The latter image (B) illustrates the remarkable uniformity of hex reconstruction induced by CO dosing.

The possibility that the CO<sub>2</sub> product of (and carbonate formed therefrom) solution CO electrooxidation in alkaline solution may also play a role in the reconstruction was checked, and eliminated, by performing parallel STM experiments with CO<sub>2</sub> rather than CO dosing. Another possibility is that the CO acts to remove residual oxygen, and thereby peroxide formed by oxygen electroreduction at negative potentials, given that adsorbed peroxide may affect the reconstruction. However, essentially identical voltammetric features, especially peak C<sub>p</sub>, were obtained for appropriately cycled surfaces in the presence as well as complete absence of oxygen in conventional electrochemical cells.

Parallel voltammetric experiments support directly the anticipated involvement of adsorbed CO in this surprising phenomenon. The quantities of irreversibly adsorbed CO present on Au(100) in 0.1 M KOH as a function of potential and dosing time were measured by transferring the electrode from CO-saturated to argon-sparged 0.1 M KOH, followed by an anodic voltammogram at 50 mV s<sup>-1</sup>. The irreversibly adsorbed CO yields a broad voltammetric peak centered at about -0.05 V (e.g., the dotted trace in Fig. 1) which allows the CO coverage,  $\theta_{CO}$ , to be evaluated given that the wave corresponds to the two-electron formation of CO<sub>2</sub> (cf ref. 13). Significantly, the  $\theta_{CO}$  values increase from about 0.1 at -0.1 V to 0.5 at -0.3 V and beyond. [These coverages were calculated with reference to the Au(100)-(1 × 1) packing density, 1.2 × 10<sup>15</sup> atoms cm<sup>-2</sup>.] While the oxidation of solution CO is initiated at substantially more negative potentials than the adsorbed species (see dashed curve in Fig. 1),

the presence of a voltammetric peak for the latter component is nonetheless evident also in the former trace.

We have embarked on a detailed investigation of CO adsorption on various gold monocrystalline surfaces using voltammetry combined with in-situ infrared spectroscopy. Another surprising observation made in the present study is the occurrence of extensive CO adsorption, deduced voltammetrically and spectroscopically, upon exposing gold surfaces to wet ambient-pressure gas-phase CO. This finding is currently under further scrutiny.

It is therefore apparent that adsorbed CO acts to facilitate the formation of uniform hex domains on Au(100). This observation is remarkable in that the adsorption of CO on (100) transition-metal surfaces in vacuum, such as Pt(100), is known to lift the hexagonal reconstruction.<sup>15</sup> On what basis, then, can we rationalize the apparently opposite, and entirely unexpected, behavior observed for the Au(100)-CO system? One relevant factor is the negative electronic charge density that is known to encourage reconstruction on Au(100) and other low-index gold electrodes, which can be understood on a theoretical basis.<sup>16</sup> Anionic adsorbates such as hydroxide considered here, as well as sulfate and halides,<sup>6,7</sup> act to lift the reconstruction on Au(100) electrodes in that the hex  $\leftrightarrow$  (1  $\times$  1) transition occurs at lower electrode potentials than in the near-absence of anion adsorption, as approximated by perchlorate electrolytes.<sup>6</sup> This latter observation correlates with the marked lowering of the potential of zero charge,  $E_{pzc}$ , brought about by anion adsorption. Given the inverted parabolic shape of the surface tension-electrode potential ( $\gamma - E$ ) curves and the displacement of the  $\gamma - E$  maximum (at  $E_{pzc}$ ) to a higher potential than for the (1  $\times$  1) surface,<sup>17</sup> one can anticipate that the hex  $\leftrightarrow$  (1  $\times$  1) "equilibrium point" would occur at electrode potentials close to  $E_{pzc}$ , the hex and (1  $\times$  1) phases being thermodynamically more stable at lower and higher potentials, respectively.<sup>6a</sup>

In contrast, adsorption of CO in bridging or other multifold geometries is known to increase the metal work function in vacuum.<sup>18</sup> As a consequence,  $E_{\text{pec}}$  is unlikely to be lowered, and quite possibly raised, by CO adsorption on Au(100). The differing effects of adsorbed halides and CO on the hex reconstruction may therefore be understandable on this basis. In both cases, however, the reconstruction dynamics are facilitated by adsorption (cf ref. 6c). This effect may be understood in terms of an increased gold surface mobility engendered by chemisorption.

#### Acknowledgments

We acknowledge discussions with Dr. Ian Tidswell. This work is supported by the U.S. Office of Naval Research and the National Science Foundation (to M.J.W.), and by the Office of Basic Energy Science, Division of Material Sciences, U.S. Department of Energy (to P.N.R.).

**References**

- (1) D.M. Kolb, in "Structure of Electrified Interfaces", P.N. Ross and J. Lipkowski, eds., VCH, New York, 1993.
- (2) M.J. Weaver and X. Gao, *Ann. Rev. Phys. Chem.*, 44 (1993), 459.
- (3) B.M. Ocko, J. Wang, A. Davenport, and H. Isaacs, *Phys. Rev. Lett.*, 65 (1990), 1466.
- (4) (a) I.M. Tidswell, N.M. Markovic, C.A. Lucas, and P.N. Ross, *Phys. Rev. B*, 47 (1993), 16542; (b) N.M. Markovic, I.M. Tidswell and P.N. Ross, *Langmuir*, submitted.
- (5) (a) X. Gao, A. Hamelin, and M.J. Weaver, *Phys. Rev. Lett.*, 67 (1991), 618; (b) X. Gao, A. Hamelin, and M.J. Weaver, *Phys. Rev. B.*, 46 (1992), 7096; (c) A. Hamelin, X. Gao, and M.J. Weaver, *J. Electroanal. Chem.*, 323 (1992), 361.
- (6) (a) X. Gao, G.J. Edens, A. Hamelin, and M.J. Weaver, *Surf. Sci.*, in press; (b) A. Hamelin, L. Stoicoviciu, G. Edens, X. Gao, and M.J. Weaver, *J. Electroanal. Chem.*, in press; (c) X. Gao and M.J. Weaver, *J. Phys. Chem.*, 97 (1993), 8685.
- (7) O.M. Magnussen, O. Hotlos, R.J. Behm, N. Batina, and D.M. Kolb, *Surf. Sci.*, in press.
- (8) (a) J. Schneider and D.M. Kolb, *Surf. Sci.*, 193 (1988), 579; (b) S-C. Chang, A. Hamelin, and M.J. Weaver, *Surf. Sci.*, 239 (1990), L543; (c) S-C. Chang, A. Hamelin, and M.J. Weaver, *J. Phys. Chem.*, 95 (1991), 5560.
- (9) A. Hamelin, M.T. Sottomayor, F. Silva, S-C. Chang, and M.J. Weaver, *J. Electroanal. Chem.*, 295 (1990), 291.
- (10) X. Gao and M.J. Weaver, *J. Electroanal. Chem.*, submitted.
- (11) R.R. Adzic, N.M. Markovic, and V.B. Vesovic, *J. Electroanal. Chem.*, 165 (1984), 105
- (12) K. Kunimatsu, A. Aramata, H. Nakajima, and H. Kita, *J. Electroanal. Chem.*, 207 (1988), 293.

- (13) S-C. Chang, A. Hamelin, and M.J. Weaver, Surf. Sci., 239 (1990), L543.
- (14) S-C. Chang, A. Hamelin, and M.J. Weaver, J. Phys. Chem., 95 (1991), 5560.
- (15) For a review see: G.A. Somorjai and M.A. Van Hove, Prog. Surf. Sci., 30 (1989), 201.
- (16) C.L. Fu and K.M. Ho, Phys. Rev. Lett., 63 (1989), 1617.
- (17) P.N. Ross and A.T. D'Agostino, Electrochim. Acta, 37 (1992), 615.
- (18) B.E. Nieuwenhuys, Surf. Sci., 105 (1981), 505.

## FIGURE CAPTIONS

### Figure 1

Cyclic voltammograms recorded at  $50 \text{ mV s}^{-1}$  for Au(100) in aqueous  $0.1 \text{ M}$  KOH. Upper and lower solid traces recorded in conventional electrochemical (argon-purged) and STM cells, respectively. Dotted upper trace: electrooxidation wave for CO irreversibly adsorbed at  $-0.5 \text{ V}$  vs SCE, after transfer to argon-purged  $0.1 \text{ M}$  KOH (see text). Dashed upper trace: electrooxidation wave for solution CO, for positive-going sweep in CO-saturated  $0.1 \text{ M}$  KOH. Current sensitivity for dashed trace one-half of that for solid and dotted trace.

### Figure 2

Typical in-situ STM images (A) ( $1 \times 1$ ) region and (B) hex domains formed on ordered Au(100) in aqueous  $0.1 \text{ M}$  KOH (see text for details).

### Figure 3

Selected members of STM image sequence for Au(100) in  $0.1 \text{ M}$  KOH, showing potential-induced development and subsequent removal of hex reconstruction: A) at  $-0.35 \text{ V}$  vs SCE, after positive potential excursion (see text). B) At  $-0.35 \text{ V}$ , 1 min after A. C) Following B, 1 min after altering potential to  $-0.7 \text{ V}$ . D) After sweeping potential positive to just beyond peak  $C_p$  (in Fig. 1).

### Figure 4

Illustrative STM images of hex domains on Au(100) in  $0.1 \text{ M}$  KOH observed at  $-0.45 \text{ V}$  following CO dosing (see text).

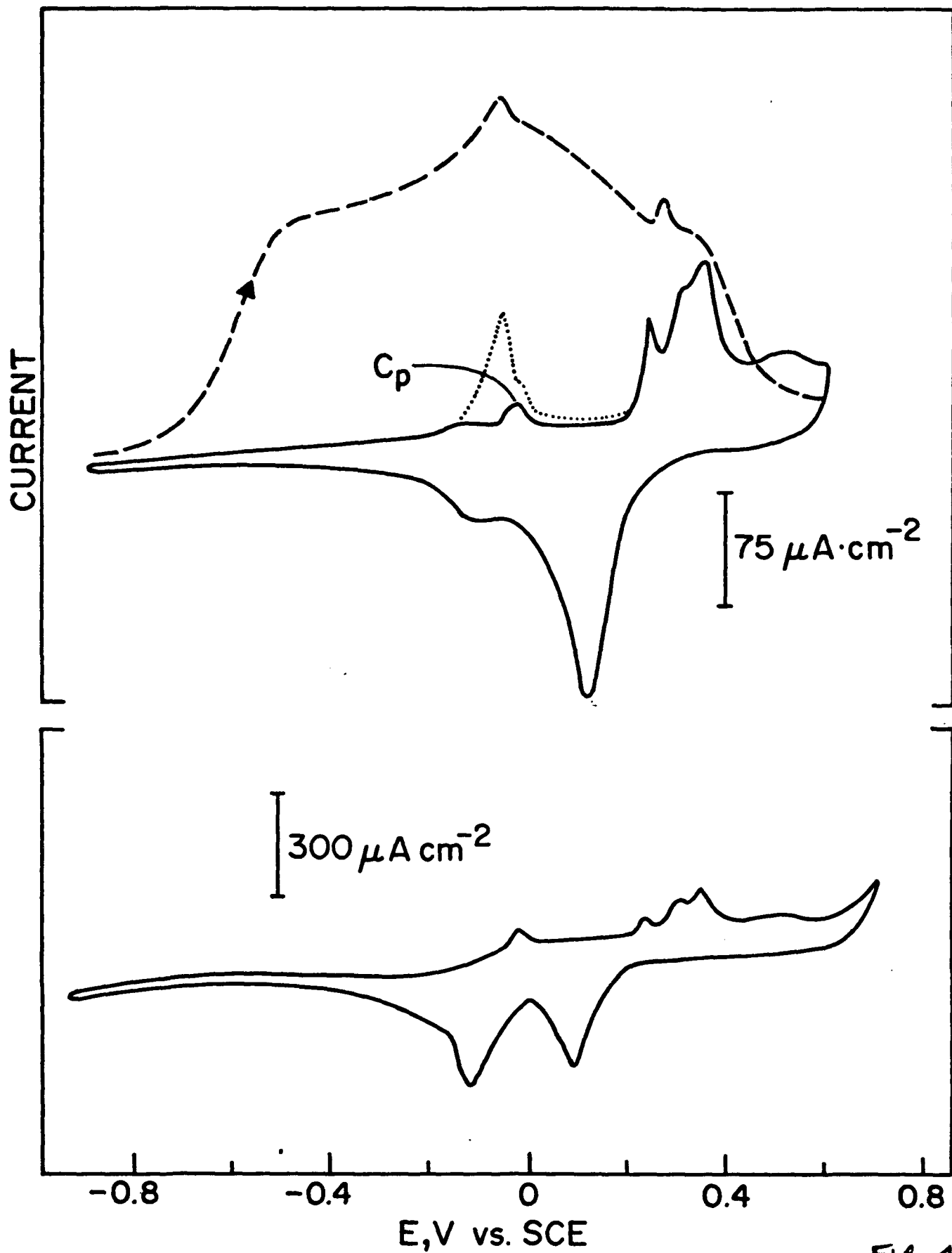
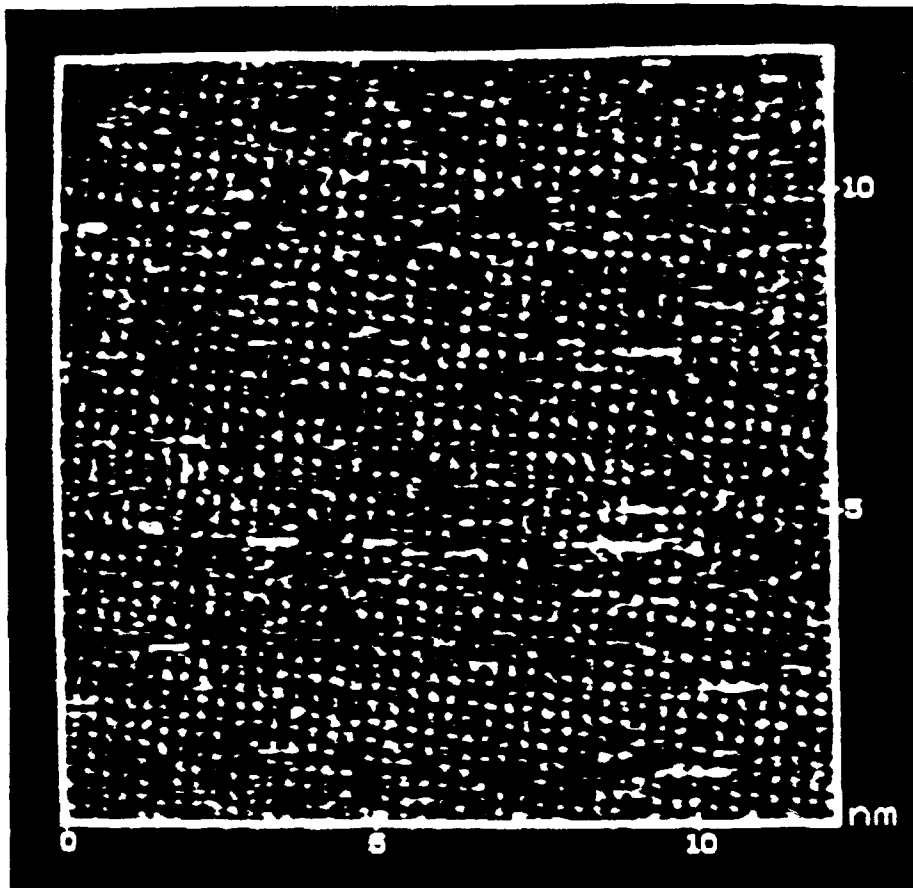
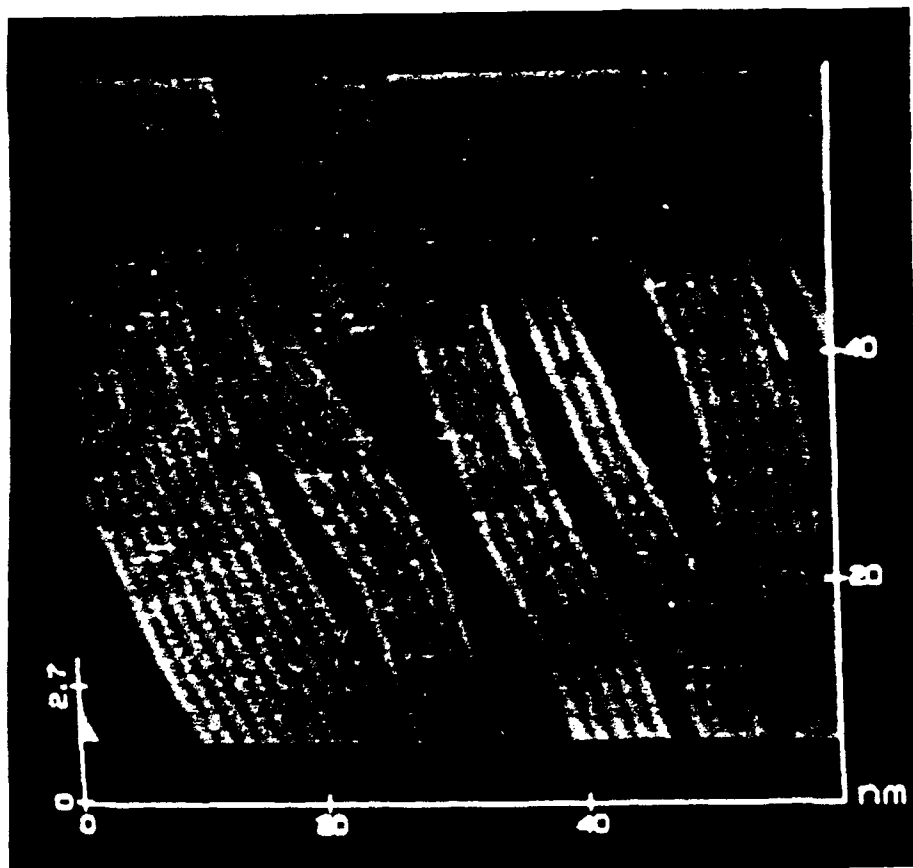


FIG 1

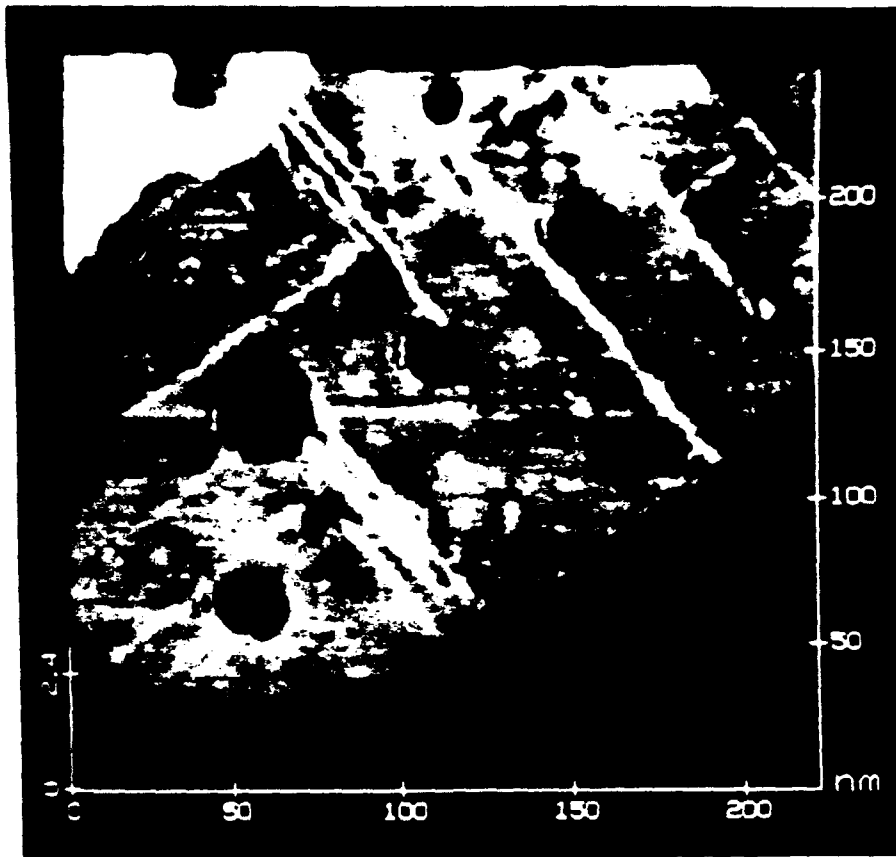


A

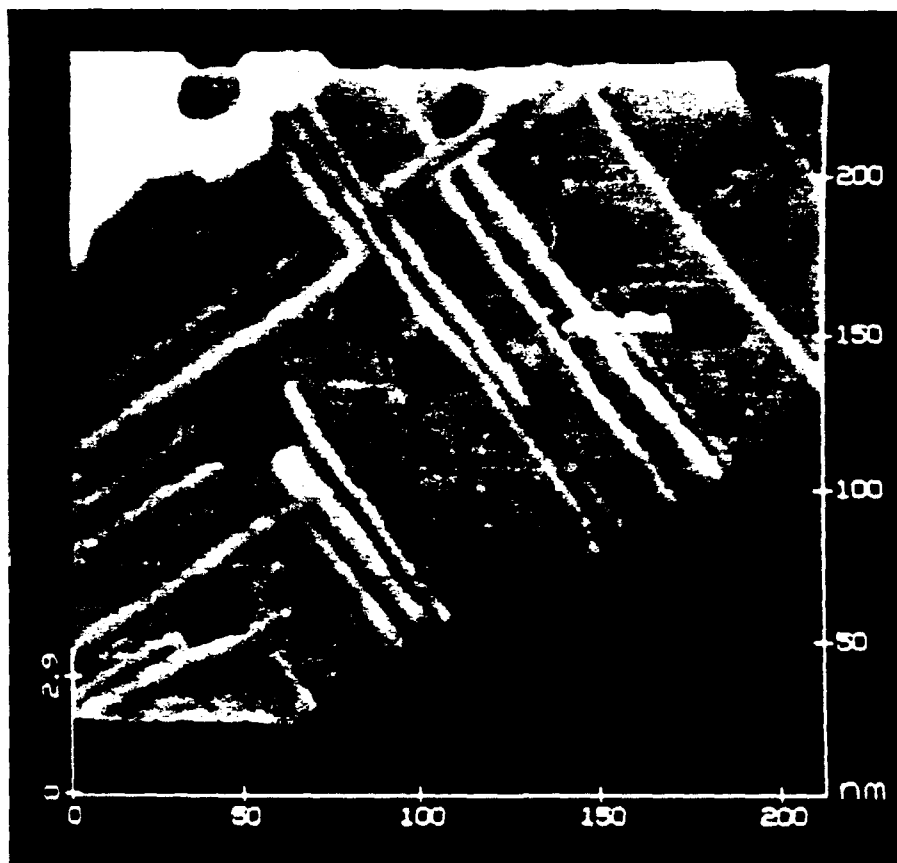


B

Fig. 2

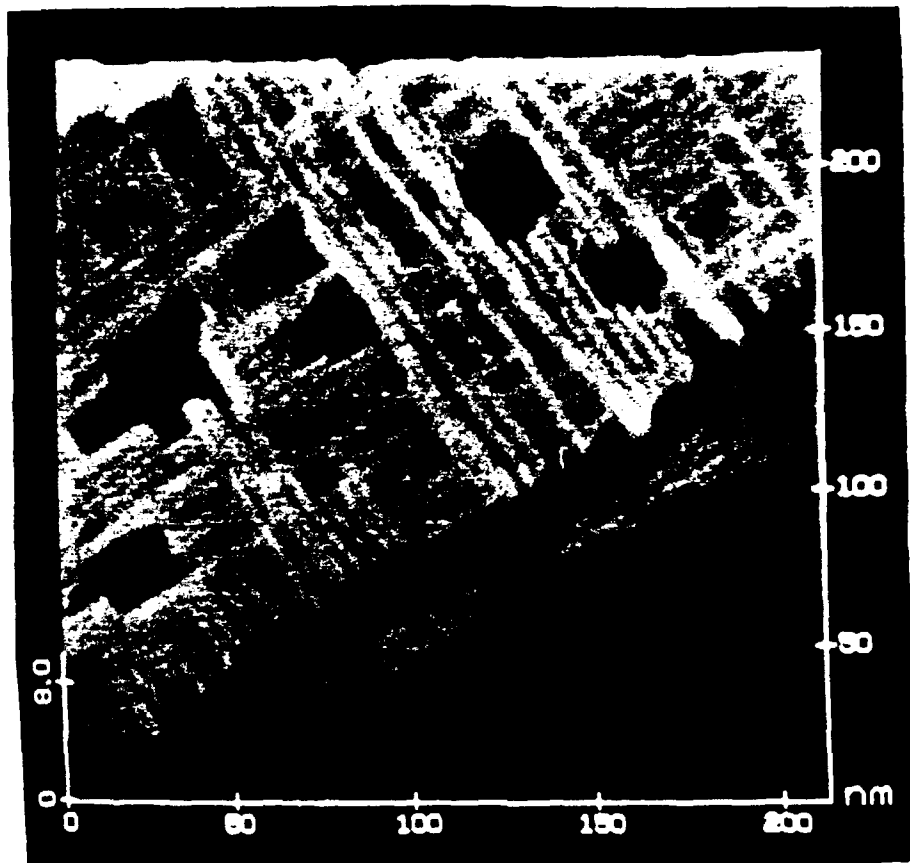


A

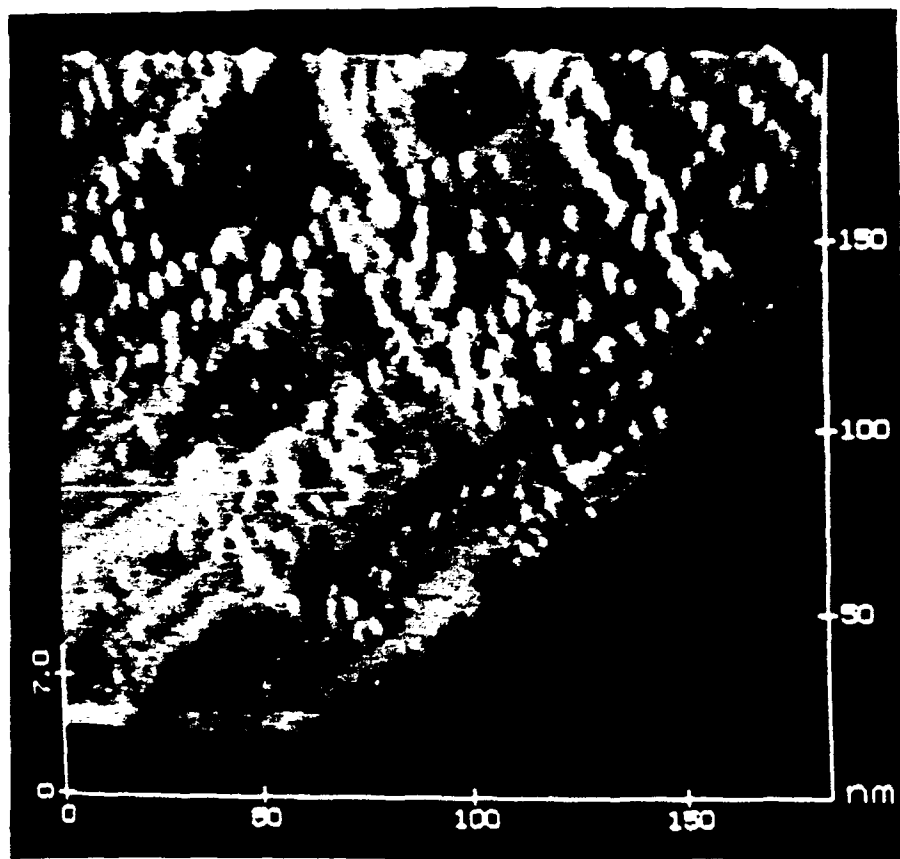


B

Fig. 3

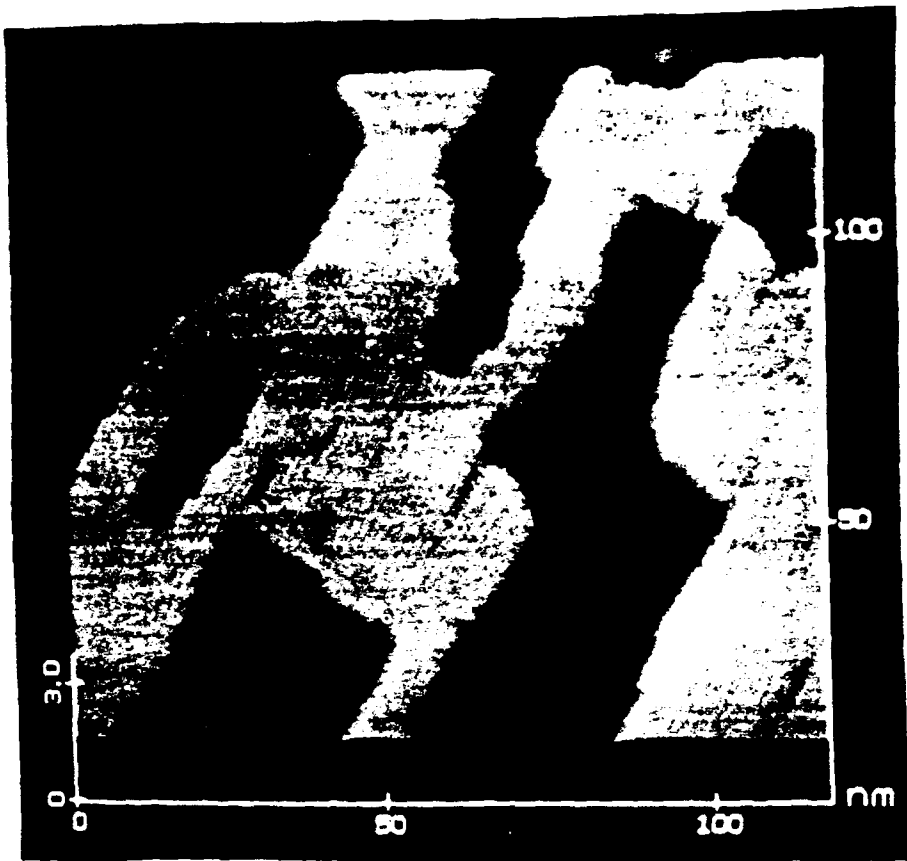


C

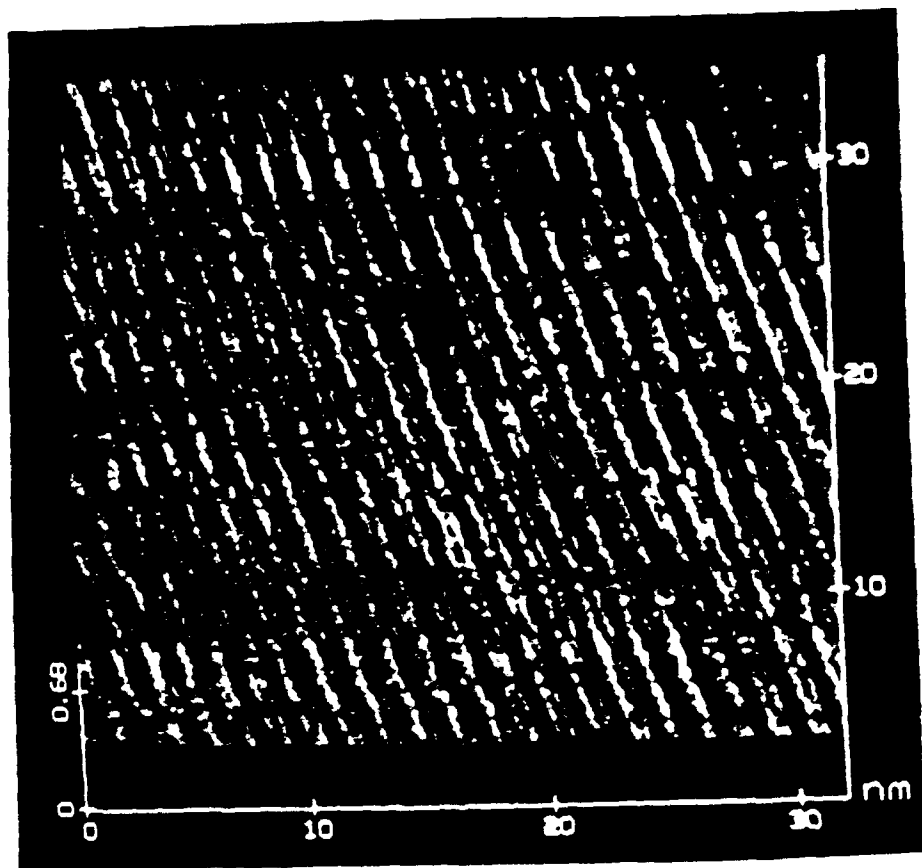


D

Fig 3  
(cont'd)



A



B

Fig. 4